Internal mode control based coordinated controller for brushless doubly fed induction generator in wind turbines during fault conditions

Ahsanullah Memon[1], Mohd Wazir Mustafa[2], Attaullah Khidrani[3], Farrukh Hafeez[4], Shadi Khan Baloch[5], Touqeer Ahmed Jumani[6]

[1,6]Department of Electrical Engineering, Mehran University of Engineering and Technology SZAB Campus, Khairpur Mirs, Pakistan
[1-4]School of Electrical Engineering, Universiti Teknologi Malaysia, Johor Bahru, Malaysia
[3]Faculty of Electrical Engineering, Balochistan University of Engineering and Technology, Khuzdar, Pakistan
[5]Department of Mechatronics Engineering, Mehran University of Engineering and Technology, Jamshoro, Pakistan

Article Info	ABSTRACT
	Brushless double fed induction generator (BDFIG) based machines have gained popularity in wind turbine applications because of their easily accessible design. Low voltage ride through (LVRT) is critical for the reliable integration of renewable energy with the power grid. Therefore, LVRT capability of brushless DFIGs makes them an attractive choice for maintaining voltage stability in grid. The existing works on BDFIG control suffer from two major drawbacks. Firstly, the methodology does not consider LVRT as a design metric, and secondly, these techniques do not have any means for coordinating between a machine side inverter (MSI) and grid side inverter (GSI). This results in sub-optimal controller design and eventually result in the violation of grid code requirements. To solve these issues, this paper proposes the use of brushless DFIGs in wind turbines using a control technique based on analytical modeling. Moreover, employing internal model control (IMC), the proposed technique can effectively coordinate the control between the MSI and GSI resulting in reduced oscillations, overshoots, and improved stability under fault conditions. Furthermore, the simulation results for wind turbine generators show that the proposed scheme significantly improves the stability and compliance of grid codes as compared to the existing hardware techniques.

Corresponding Author:

Ahsanullah Memon
Department of Electrical Engineering
Universiti Teknologi Malaysia, Malaysia
Email: memon.ahsanullah@graduate.utm.my

1. INTRODUCTION

The increasing demand for electric power has spurred the growth of renewable energy (RE) sources such as solar and wind energy [1]. Wind farms have received much attention over the last decade due to the abundance of natural wind in many parts of the world. Although, RE has an important role to play in the future of sustainable cities. However, to reliably integrate RE sources into the power grid, certain challenges and problems need to be addressed [2], [3]. The absence of motors in photo-voltaic (PV) based sources makes them simple to integrate into the power grid, which is also one of the factors of their popularity [4]. However, to utilize wind energy, one needs to install induction generators on the wind turbines which makes

the task of interfacing wind turbines to the power grid more challenging, i.e., regulating and conditioning of the power, voltage, and frequency with high efficiency and flexibility [5], [6].

Low voltage ride through (LVRT), also referred to as fault ride through, represents the capability of electrical energy generators to remain connected to the power grid during short periods of lower electric network voltage, i.e., voltage dips [7], [8]. The main motivation behind having generators with good LVRT capabilities is to prevent widespread loss of generation caused by a short circuit at high voltage (HV) or extremely high voltage (EHV) levels [9], [10]. The winding current in a generator is responsible to maintain a magnetic field and in turn a minimum voltage to operate the generator. However, if this voltage drops below a certain level, the generator may not work correctly and even disconnect from the power grid. This may result in a cascading failure leading to blackouts [11]. This problem becomes even more challenging in double fed induction generators (DFIGs) due to the presence of two sets of powered magnetic windings [12]. Existing works on the use of DFIGs focus on the high energy capture efficiency and improved power quality without due consideration to the fact that DFIGs may not have the desired LVRT characteristics in terms of grid code requirements [13].

Although brushless double fed induction generators (BDFIGs) are gaining popularity among commercial applications in wind turbines, research on investigating and improving the LVRT capabilities of BDFIGs is very limited. To solve this issue, this paper focuses on developing a robust control technique for BDFIG based wind turbines that can improve the LVRT characteristics of the generator in the presence of voltage dips. The proposed technique is based on an analytical model of a BDFIG to capture a BDFIG based machine's system dynamics, and using a coordinate strategy between a machine side inverter (MSI) and grid side inverter (GSI), the direct current (DC) link voltage is controlled by injecting reactive current into the grid by the GSI to avoid a large-scale blackout. This is achieved by employing IMC-based feed-forward tuning of MSI parameters. Moreover, to reduce the effect of unknown disturbances due to a process-model mismatch in the analytical model, internal model control (IMC) also helps to reduce oscillations. Thus, the proposed control technique results in a robust controller.

The main contributions of this paper are as follows: 1) An analytical model-based control combined with an IMC-based coordinated controller to optimize the PI values of the generator at the time of a fault reducing the oscillations, and thus, providing grid support during faults. In particular, the proposed technique improves the LVRT capabilities of a grid-connected inverter to avoid disconnection of grids. 2) A thorough simulation-based study to investigate LVRT in BDFIG based wind turbines and evaluate the effectiveness of the proposed controller. The rest of the paper is organized as follows: section 1 provides a background for this paper. Section 2 presents the proposed control technique and the simulation results are discussed in section 3. The paper is concluded in section 4.

2.   INTRODUCTION OF BDFIG

The basic structure of a BDFIG based wind turbine is shown in Figure 1. A BDFIG is connected to the mechanical shaft system of the wind turbine. Unlike DFIGs, a BDFIG consists of two magnetically and electrically uncoupled stator windings with a well-defined rotor structure [14]. The stator winding which is directly connected to the grid is called the power-winding (PW) while the other which is connected to the grid through a power electronic (PE) converter is called the control winding (CW) [15]. The most commonly used construction for BDFIGs is the nested-loop rotor construction [16]. In this construction, aluminum or copper bars are used to create many nests with multiple loops. A rotating magnetic field wave is then generated in the air-gap by the two stator windings, as seen from the rotor.

To enable vector control of the machine, the PW and CW voltages are translated into the dqz reference frame. Note that, the dq reference frame is aligned with the PW flux orientation [17], [18]. The resulting dq components for PW given the PW current I_p are as follows:

$$V_{pd} = I_{pd}R_{sp} - j\omega_p\lambda_{pq} + \frac{d\lambda_{pd}}{dt} \tag{1}$$

$$V_{pq} = I_{pq}R_{sp} - j\omega_p\lambda_{pd} + \frac{d\lambda_{pq}}{dt} \tag{2}$$

$$\lambda_{pd} = L_{sp}I_{pd} + L_{hp}I_{rd} \tag{3}$$

$$\lambda_{pq} = L_{sp}I_{pq} + L_{hp}I_{rq} \tag{4}$$

where, V_{pd} and V_{pq} denote the d and q components of PW voltage while λ_{pd} and λ_{pq} denote the d and q components of PW flux [19]. Similarly, for the d and q components for CW given CW current I_c we have:

$$V_{cd} = I_c R_{sc} - j(\omega_p - N_r \omega_r)\lambda_{cq} + \frac{d\lambda_{cd}}{dt} \tag{5}$$

$$V_{cq} = I_c R_{sc} - j(\omega_p - N_r \omega_r)\lambda_{cd} + \frac{d\lambda_{cq}}{dt} \tag{6}$$

$$\lambda_{cd} = L_{sc} I_{cd} + L_{hc} I_{rd} \tag{7}$$

$$\lambda_{cq} = L_{sc} I_{cq} + L_{hc} I_{rq} \tag{8}$$

where, V_{cd} and V_{cq} denote the d and q components of CW voltage while λ_{cd} and λ_{cq} denote the d and q components of CW flux. Similarly, for the d and q components for rotor given rotor current I_r we have:

$$V_{rd} = 0 = I_{rd} R_r - j(\omega_p - P_p \omega_r)\lambda_{rq} + \frac{d\lambda_{rd}}{dt} \tag{9}$$

$$V_{rq} = 0 = I_{rq} R_r - j(\omega_p - P_p \omega_r)\lambda_{rd} + \frac{d\lambda_{rq}}{dt} \tag{10}$$

$$\lambda_{rd} = L_{hp} I_{pd} + L_{hc} I_{cd} + L_r I_{rd} \tag{11}$$

$$\lambda_{rq} = L_{hp} I_{pq} + L_{hc} I_{cq} + L_r I_{rq} \tag{12}$$

where, V_{rd} and V_{rq} denote the d and q components of rotor voltage while λ_{rd} and λ_{rq} denote the d and q components of rotor flux. Finally, the rotor torque can be calculated as follows;

$$T_e = -\frac{3}{2} P_p I_m [\lambda_p{}^* I_p] - \frac{3}{2} P_c I_m [\lambda_c{}^* I_c] \tag{13}$$
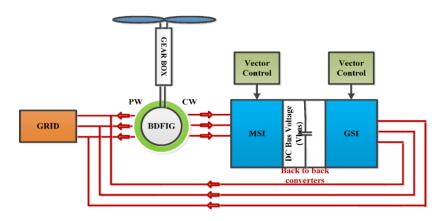

Figure 1. System model

3. PROPOSED CONTROL TECHNIQUE

A vector controller oriented on the PW reference frame is proposed to regulate the speed and reactive power independently [20]. The reactive power and speed are calculated analytically using the mathematical model of BDFIM while the PI controller gains are derived through the IMC method [21]. In the vector control scheme, the dq components of PW and CW currents are regulated to obtain the desired reactive power and speed of the machine. The controlled signal obtained after conversion from dq to abc is fed to the pulse width modulation (PWM) block which accordingly switches the inverter to inject the controlled amount of power into the grid [22]. It is important to note that the current study utilizes only mesenchymal stem cell (MSC) to regulate the speed and reactive power of the machine.

3.1. Machine side inverter

The MSI is directly connected to the CW and is responsible for controlling the active and reactive powers using the d and q components, respectively [23]. Using (1) to (2), we can derive a non-linear dynamic model for a BDFIG which also shows the relationship between the two stator-windings, i.e., PW current is regulated using the CW current because of cross-coupling. Thus, the transfer function for CW voltage is given by:

$$v_c = \alpha_1 I_c + \alpha_2 \frac{dI_c}{dt} \tag{14}$$

where, $\alpha_1, \alpha_1, \ldots \ldots \alpha_4$ denote the open-loop coefficients for CW current control.

Thus, we now have the system transfer functions for voltage and current. To handle external disturbances, we introduce feed-forward compensation. Feed-forward compensation is typically used to handle external disturbances. However, if the transfer function is not an exact match of the process to be controlled, feed-forward compensations may lead to oscillations and stability issues. Therefore, in this paper, we propose the use of IMC to improve system stability by capturing external disturbances [21]. Thus, the MSI using the IMC method is shown in Figure 2. The resulting gain values using IMC are as follows:

$$K_p^{PW} = 2\pi B_p \beta_2 \quad , \quad K_i^{PW} = 2\pi B_p \beta_1, K_p^{CW} = 2\pi B_c \alpha_2 , K_i^{CW} = 2\pi B_c \alpha_1$$

where, K_p^{PW} , K_i^{PW} and K_p^{CW}, K_i^{CW} denote the gain values for PW and CW current, respectively. Similarly, B_p and B_c represent the frequency bandwidth for PW and CW, respectively.
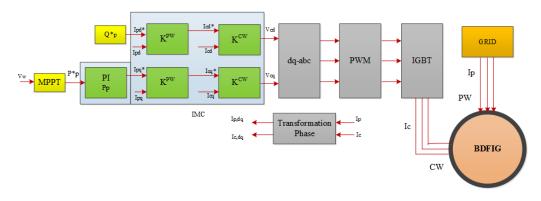

Figure 2. Machine side inverter

3.2. Grid side converter

The DC-link voltage overshoots as soon as a fault occurs leading to undesirable consequences [24]. To avoid such problems and improve compliance with the grid code requirements, we introduce the second type of controller used in the proposed technique called the grid side inverter (GSI) [25]. The GSI is used to control the DC-link voltage and reactive power (set to zero). In typical power grids, a voltage dip may cause critical machine parameters such as active/reactive power, torque, and DC-link voltage to become unstable. To solve this issue, we propose a coordinated strategy between the MSI and GSI controllers. Using a similar approach to MSI, the GSI controller is shown in Figure 3.
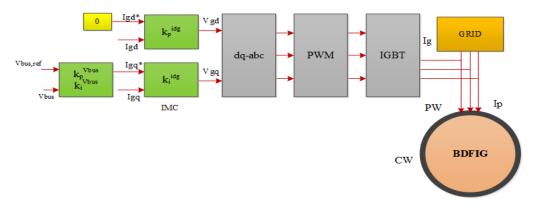

Figure 3. Grid side inverter

The gains for the GSI using the IMC method are as follows:

$$K_p^{idg} = 2B_{dc}L_g - R_g \quad , \quad K_i^{idg} = 2B_{dc}^2 L_g$$

where, B_{dc}, L_g, and R_g represent DC-link voltage bandwidth, GSI choke inductance, and GSI choke resistance, respectively. Moreover, the tuning parameters for the voltage bus regulators are set as follows:

$$K_p^{Vbus} = -580, K_i^{Vbus} = -8000$$

4. RESULTS AND DISCUSSION

To evaluate the effectiveness of the proposed technique, we simulated the model in MATLAB/SIMULINK. In this system model, we have two control loops are simulated, i.e., the power loop (outer loop) and current loop (inner loop). The dq components of CW current are generated by the outer loop while the dq components of the CW voltage are generated by the inner loop. The maximum power point tracking (MPPT) algorithm was used to obtain the reference value of active power and the reference value of reactive power is determined using grid codes. A fault condition was simulated at $t = 2$ seconds. The proposed control technique is compared with the contemporary approach, i.e., using an MSI with a crowbar design. We evaluate the proposed technique using the following three important metrics:

4.1. Current response

Symmetrical faults in the power grid lead to increased machine currents which may cause damage to equipment and loss of capital. For example, an Insulated-gate bipolar transistor (IGBT) can withstand 2 per unit CW current for a 1 ms time period [26]. The proposed technique limits the CW current within the specified tolerance levels by improved PI tuning using IMC at the MSI and injecting reactive current to the grid using the GSI. Figure 4 shows the flux response of CW and PW currents and the PW Flux. Figures 4 (a) and 4 (b) show that the proposed controller successfully manages to keep the machine currents within the allowed range even in the presence of a fault at $t = 2$ seconds.
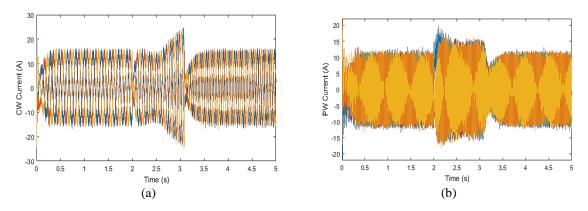

Figure 4. These figures are; (a) CW current and (b) PW current

4.2. Power response

The proposed technique uses an active approach to control active as well as reactive power using PW currents I_{pd} and I_{pq}, respectively. Note that contemporary approaches in most of the existing literature consider only active power control. Figure 5 presents the active and reactive power responses for the proposed technique and contemporary approach. The activation of the crowbar makes the power electronic converter deactivated for the time which is counted as the main disadvantage of the crowbar. Crowbar also causes to oscillate the machine and makes it an ordinary machine as shown in the figure. It is observed that the proposed technique results in significantly lower oscillations and overshoot time in the presence of faults. The various system dynamics are given in Table 1.

Table 1. Comparison of system dynamics

	POR (%)	tr*	ts*
Active Power			
Contemporary approach	16.28	164.22	270.54
Proposed technique	13.94	32.53	52.27
Improvement	14.5%	80%	81.5%
Reactive Power			
Contemporary approach	19.33	148.66	223.67
Proposed technique	16.28	24.45	39.45
Improvement	15.78%	83.55%	82.36%
POR: Peak Overshoot Ratio, tr: rise time, ts: setting time.			

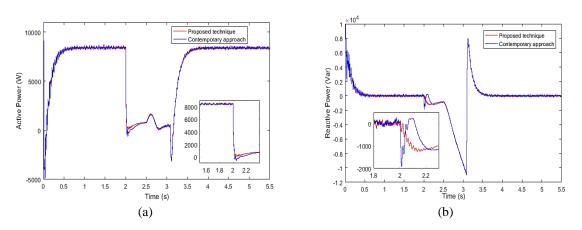(a)   (b)

Figure 5. These figures are; (a) active power response and (b) reactive power response

4.3. DC-link voltage

To appreciate the effect of GSI in LVRT conditions, Figure 6 presents the DC link voltage during the fault at $t = 2$ seconds. We observe that the proposed technique is significantly more robust than the contemporary approach of using a crowbar. The system dynamics during the fault condition are given in Table 2. We observe a 25equa% faster recovery time and a 41.2% smaller peak overshoot ratio (POR) which will prevent the proposed controller from being disconnected to the grid. It is obvious that the introduction of a GSI injecting reactive power to the grid using IMC control during faults results in improved system dynamics and the voltage dip does not enter the critical region where the controller may get disconnected from the grid.

Figure 6. DC bus voltage response

Table 2. Comparison of system dynamics

	POR (%)	tr*	ts*
Contemporary approach	26.7	0.22	0.8
Proposed technique	15.7	0.2	0.6
Improvement	41.20%	9.09%	25%

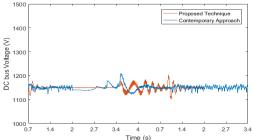### 5. CONCLUSION

This paper presented a coordinated control technique for low voltage ride through under fault conditions in grid-connected microgrids. The proposed technique was designed for wind turbines using brushless doubly-fed induction generators. Using a crowbar-less approach, the proposed technique improves the coordination between GSI and MSI by tuning the MSI gains using the IMC method. Thus, when a voltage dip occurs, the MSI gains are tuned to cause the CW current to control the reactive power fed by the GSI to the grid. Therefore, during a fault, the GSI provides reactive power to the grid by controlling the PW current using the CW current at MSI. Simulations on MATLAB show that the BDFIG can not only successfully ride through fault conditions but it can do so 25% faster as compared to existing techniques using a crowbar. Moreover, the system dynamics for active and reactive power are also significantly improved.

REFERENCES

[1] G. S. Kaloi, J. Wang, and M. H. Baloch, "Study of stabilty analysis of a grid connected doubly fed induction generator based on wind energy application," *Indones. J. Electr. Eng. Comput. Sci.*, vol. 3, no. 2, pp. 305–313, 2016, doi: 10.11591/ijeecs.v3.i2.pp305-313.

[2] A. Khidrani, M. H. Habibuddin, M. W. Mustafa, M. N. Aman, and A. S. Mokhtar, "A hybrid voltage-current compensator using a synchronous reference frame technique for grid-connected microgrid under nonlinear load conditions," *Int. Trans. Electr. Energy Syst.*, vol. 30, no. 10, p. e12530, Oct. 2020, doi: 10.1002/2050-7038.12530.

[3] T. A. Jumani, M. . Muatafa, N. Hamadneh, and S. Atawneh, "Computational intelligence-based optimization methods for power quality and dynamic response enhancement of ac microgrids," *Energies*, vol. 13, no. 1, pp. 1-22, Aug. 2020, doi: 10.3390/en13164063.

[4]   T. A. Jumani, M. W. Mustafa, M. M. Rasid, N. H. Mirjat, Z. H. Leghari, and M. Salman Saeed, "Optimal voltage and frequency control of an islanded microgrid using grasshopper optimization algorithm," *Energies*, vol. 11, no. 11, 2018, doi: 10.3390/en11113191.

[5]   T. A. Jumani, M. W. Mustafa, A. S. Alghamdi, M. M. Rasid, A. Alamgir, and A. B. Awan, "Swarm Intelligence-Based Optimization Techniques for Dynamic Response and Power Quality Enhancement of AC Microgrids: A Comprehensive Review," *IEEE Access*, vol. 8, pp. 75986–76001, 2020, doi: 10.1109/ACCESS.2020.2989133.

[6]   P. Pura and G. Iwanski, "Direct torque control of a doubly fed induction generator working with unbalanced power grid," *Int. Trans. Electr. Energy Syst.*, vol. 29, no. 4, p. e2815, Apr. 2019, doi: 10.1002/etep.2815.

[7]   O. O. Mohammed, M. W. Mustafa, and M. N. Aman, "A Graph-Theoretic Approach to Capacity Benefit Margin Calculation for Large Multiarea Power Systems," *IEEE Syst. J.*, vol. 14, no. 1, pp. 1230–1233, Mar. 2020, doi: 10.1109/JSYST.2019.2910554.

[8]   S. A. Taher, Z. Dehghani Arani, M. Rahimi, and M. Shahidehpour, "A new approach using combination of sliding mode control and feedback linearization for enhancing fault ride through capability of DFIG-based WT," *Int. Trans. Electr. Energy Syst.*, vol. 28, no. 10, p. e2613, Oct. 2018, doi: 10.1002/etep.2613.

[9]   O. O. Mohammed, M. W. Mustafa, M. N. Aman, S. Salisu, and A. O. Otuoze, "Capacity benefit margin assessment in the presence of renewable energy," *Int. Trans. Electr. Energy Syst.*, vol. 30, no. 9, Sep. 2020, doi: 10.1002/2050-7038.12502.

[10] M. N. F. Nashed, M. N. Eskander, and M. A. Saleh, "Mitigation of faults in grid-connected wind-driven single machine brushless double-fed induction generator," *Indones. J. Electr. Eng. Comput. Sci.*, vol. 15, no. 3, pp. 1178–1188, 2019, doi: 10.11591/ijeecs.v15.i3.pp1178-1188.

[11] M. Tsili and S. Papathanassiou, "A review of grid code technical requirements for wind farms," *IET Renew. Power Gener.*, vol. 3, no. 3, p. 308, 2009, doi: 10.1049/iet-rpg.2008.0070.

[12] R. M. Monteiro Pereira, A. J. C. Pereira, C. M. Ferreira, and F. P. Maciel Barbosa, "Influence of crowbar and chopper protection on DFIG during low voltage ride through," *Energies*, vol. 11, no. 4, 2018, doi: 10.3390/en11040885.

[13] Y. M. Alsmadi *et al.*, "Detailed Investigation and Performance Improvement of the Dynamic Behavior of Grid-Connected DFIG-Based Wind Turbines Under LVRT Conditions," *IEEE Trans. Ind. Appl.*, vol. 54, no. 5, pp. 4795–4812, 2018, doi: 10.1109/tia.2018.2835401.

[14] F. Zhang, T. Tong, and H. Liu, "Design and analysis of 50KW dual-stator brushless doubly-fed generator for wind turbine," *2017 20th Int. Conf. Electr. Mach. Syst. ICEMS 2017*, 2017, doi: 10.1109/ICEMS.2017.8056427.

[15] S. Abdi, A. Grace, E. Abdi, and R. McMahon, "A new optimized rotor design for brushless doubly fed machines," *2017 20th International Conference on Electrical Machines and Systems (ICEMS)*, 2017, doi: 10.1109/ICEMS.2017.8056048.

[16] S. Abdi, E. Abdi, and R. McMahon, "A Light-Weight Rotor Design for Brushless Doubly Fed Machines," in *Proceedings - 2018 23rd International Conference on Electrical Machines, ICEM 2018*, Oct. 2018, pp. 493–498, doi: 10.1109/ICELMACH.2018.8507156.

[17] J. Poza, E. Oyarbide, D. Roye, and M. Rodriguez, "Unified reference frame dq model of the brushless doubly fed machine," *IEE Proc. Electr. Power Appl.*, vol. 153, no. 5, pp. 726–734, 2006, doi: 10.1049/ip-epa:20050404.

[18] S. Shao, E. Abdi, F. Barati, and R. McMahon, "Stator-Flux-Oriented vector control for brushless doubly fed induction generator," *IEEE Trans. Ind. Electron.*, vol. 56, no. 10, pp. 4220–4228, 2009, doi: 10.1109/TIE.2009.2024660.

[19] Y. Liu, W. Xu, K. Yu, and F. Blaabjerg, "A new vector control of brushless doubly-fed induction generator with transient current compensation for stand-alone power generation applications," in *Conference Proceedings - IEEE Applied Power Electronics Conference and Exposition - APEC*, Apr. 2018, vol. 2018-March, pp. 1392–1398, doi: 10.1109/APEC.2018.8341199.

[20] G. Joshi and P. Pius, "ANFIS controller for vector control of three phase induction motor," *Indones. J. Electr. Eng. Comput. Sci.*, vol. 19, no. 3, pp. 1177–1185, 2020, doi: 10.11591/ijeecs.v19.i3.pp1177-1185.

[21] M. Su, W. Jin, G. Zhang, W. Tang, and F. Blaabjerg, "Internal model current control of brushless doubly fed induction machines," *Energies*, vol. 11, no. 7, 2018, doi: 10.3390/en11071883.

[22] A. Zhang *et al.*, "Crowbarless Symmetrical Low-Voltage Ride through Based on Flux Linkage Tracking for Brushless Doubly Fed Induction Generators," *IEEE Trans. Ind. Electron.*, vol. 67, no. 9, pp. 7606–7616, Sep. 2020, doi: 10.1109/TIE.2019.2944096.

[23] F. K. Moghadam, S. Ebrahimi, A. Oraee, and J. M. Velni, "Vector control optimization of DFIGs under unbalanced conditions," *Int. Trans. Electr. Energy Syst.*, vol. 28, no. 8, p. e2583, Aug. 2018, doi: 10.1002/etep.2583.

[24] T. L. Van, T. H. Truong, H. Tran, and N. K. Dang, "A Coordinated Control Strategy for DC-link Voltage and Crowbar to Enhance Low Voltage Ride-Through of DFIG-based Wind Energy Conversion Systems," *2018 4th Int. Conf. Green Technol. Sustain. Dev.*, pp. 164–168, 2018.

[25] J. Yao, H. Li, Y. Liao, and Z. Chen, "An Improved Control Strategy of Limiting the DC-Link Voltage Fluctuation for a Doubly Fed Induction Wind Generator," *IEEE Transactions on Power Electronics*, vol. 23, no. 3, pp. 1205–1213, 2008.

[26] H. Geng, C. Liu, and G. Yang, "LVRT capability of DFIG-based WECS under asymmetrical grid fault condition," *IEEE Trans. Ind. Electron.*, vol. 60, no. 6, pp. 2495–2509, 2013, doi: 10.1109/TIE.2012.2226417.